2024-1356 IJOI
https://www.ijoi-online.org/

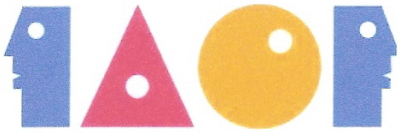

MAJOR CAUSE OF SUBSIDENCE OF ADJACENT BUILDINGS DURING FOUNDATION EXCAVATION

Tse-Shan Hsu
President, Institute of Mitigation for Earthquake Shear Banding Disasters
Professor, Feng-Chia University, Taiwan, R.O.C., tshsu@fcu.edu.tw

Yan-Ming Wang
Director, Institute of Mitigation for Earthquake Shear Banding Disasters, Taiwan, R.O.C.

Yu-Chien Wu
Ph.D. Student, Ph.D. Program for Infrastructure Planning and Engineering,
Feng-Chia University, Taiwan, R.O.C.

Zong-Lin Wu
Assistant Professor, National Chin-Yi University of Technology, Taiwan, R.O.C.

Abstract

In the past, technicians have used Terzaghi's safety factor formula to calculate resistance to piping failure in the design of retaining walls for adjacent buildings within excavation areas and to evaluate the collapse potential due to piping failure. However, during foundation excavation, retaining walls that are assessed as not susceptible to piping failure do experience such failure. In view of this, this paper presents a literature review and a case study involving two distinct piping failure mechanisms to identify the reason for the collapse of adjacent buildings due to piping failure in retaining walls during foundation excavation. The findings reveal that: (1) during foundation excavation, piping failure exclusively occurs within shear bands; (2) piping is inherently a non-steady-state mass-non-conserving pipe flow, rather than a steady-state mass-conserving seepage; (3) when piping occurs, groundwater sequentially transports soils including silt, sand, and gravel, spurting out towards the excavation surface through outlets formed by the pore spaces in

shear bands; (4) after the failure of the retaining wall due to piping, a piping hole appears in the back of the wall, leading to notable subsidence of buildings above the location of the piping hole. Based on the findings, the authors suggest that the design of retaining walls for foundation excavation should incorporate an unsteady-state mass-non-conserving piping mechanism. This approach will enable technicians to accurately assess the piping failure potential of retaining walls, thereby ensuring the safety of both the retaining walls and adjacent buildings during foundation excavation.

Keywords: retaining wall, piping failure, shear banding, foundation excavation.

Introduction

In the process of designing retaining walls, in addition to satisfying the existing design specifications of the walls, technicians must ensure that retaining wall piping failures, such as the Taiwanese examples shown in Figures 1 to 3, do not occur.

Figure 1 shows the piping failure of the retaining wall in the open-cut tunnel on the Central Cross Highway in Taichung. Figure 2 shows the piping failure of the gabion retaining wall along the bank of Toubiankeng Creek in Taichung. Figure 3 shows the piping failure of the retaining walls on both sides of the Gangweigou Creek floodway in Tainan.

Figure 1. Piping failure of the retaining wall of the open-cut tunnel (Central Cross Highway in Taichung, Taiwan).

Figure 2. Piping failure of the gabion retaining wall
(Toubiankeng Creek in Taichung, Taiwan).

Figure 3. Piping failure of the retaining walls on both sides of the floodway
(Gangweigou Creek in Tainan, Taiwan).

Evidently, piping can easily induce retaining wall failure. Currently, technicians use the formula proposed by Terzaghi to evaluate piping failure potential in retaining wall design and ensure that retaining walls do not experience piping failure. However, piping failure often occurs in various forms of retaining walls. Therefore, in this paper, the authors first present the two piping failure mechanisms proposed by Terzaghi (1943) and Hsu et al. (2020) and then a case study to demonstrate that only the piping failure mechanism proposed by Hsu et al. (2020) is consistent with real-world scenarios.

Literature Review

Piping Failure Mechanism Proposed by Terzaghi

In 1943, Terzaghi, recognized as the father of soil mechanics, proposed the piping failure mechanism of sheet pile retaining walls during foundation excavation when the groundwater tables on either side of the retaining wall are different, and he derived a formula to calculate the safety factor against piping failure based on this mechanism.

Figure 4 shows the flow net of seepage used by Terzaghi in deriving the formula. The embedding depth of the sheet pile retaining wall is denoted by D, the foundation excavation depth is denoted by D_1, the elevation difference of the groundwater tables on either side of the sheet pile retaining wall is denoted by h_1, the total thickness of the permeable layer below the excavation surface is denoted by D_2, and the area of excavation surface that is heaved due to piping is within a distance $D/2$ from the wall surface of the sheet pile retaining wall.

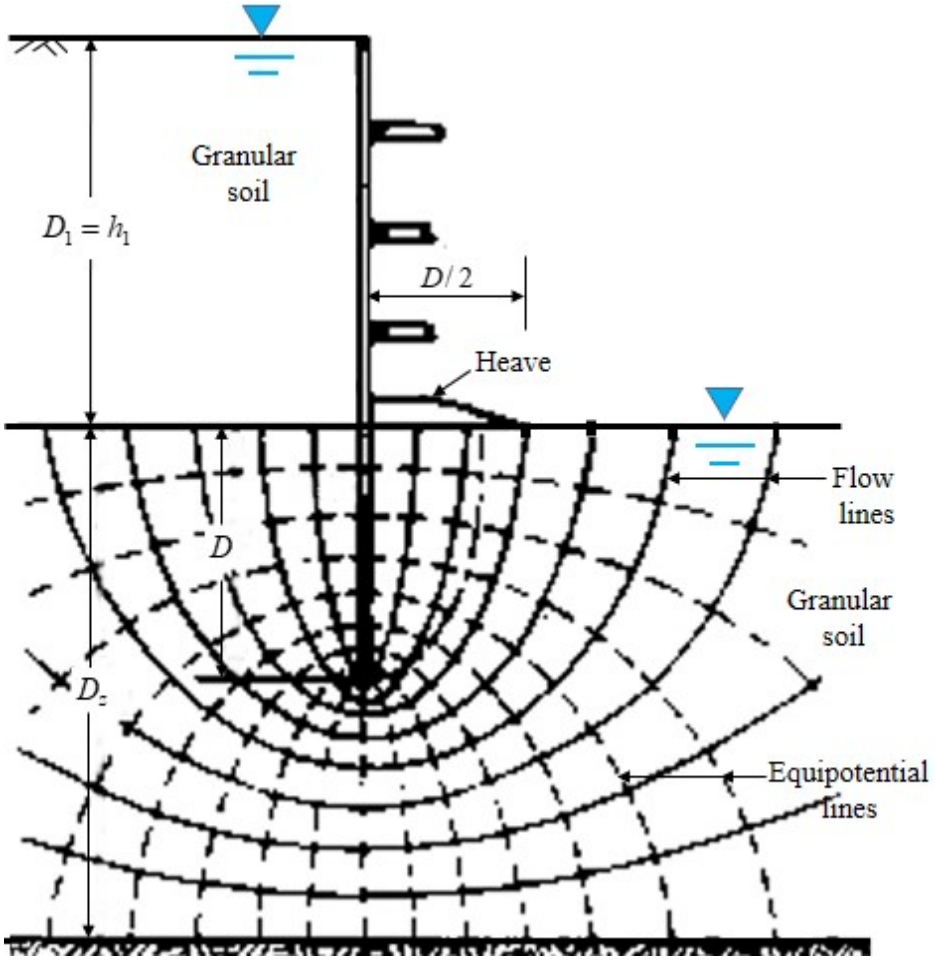

Figure 4. Grid composed of seepage lines and equipotential lines for a sheet pile retaining wall as excavation support (Terzaghi, 1943).

Figure 5 shows the effective weight *W'* of the soil column submerged in groundwater and the upward buoyancy force U_s acting on the bottom surface of the soil column depicted in the seepage grid shown in Figure 4. Terzaghi defined the piping resistance safety factor, *FS*, as

$$FS = W'/U_s \quad (1)$$

Terzaghi considered piping failure to occur when $FS < 1.0$.

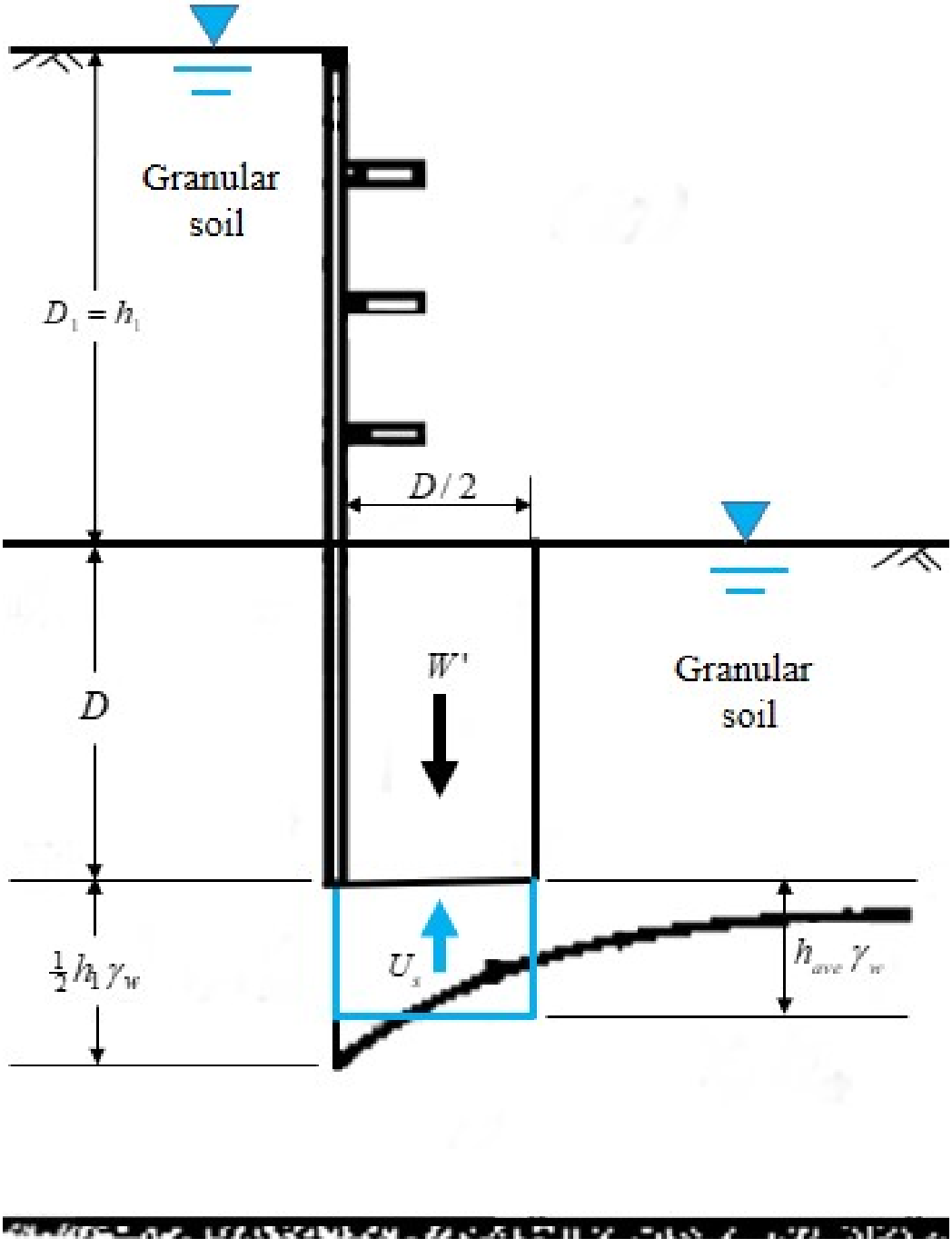

Figure 5. W' and U_s used to determine the safety factor against piping (Terzaghi, 1943).

When the excavation depth is D_1, the elevation difference of the groundwater tables on either side of the sheet pile retaining wall is h_1, the thickness of the permeable layer below the excavation surface is D_2, and the average water head of the equal potential energy line passing through the bottom of the soil column is h_{ave}, Terzaghi posited that piping failure can cause heaving of the excavation surface; the area of the block inducing the heave of the excavation surface encompasses the embedding depth D of the retaining wall below the excavation surface and the distance $D/2$ from the wall surface of the sheet pile retaining wall in the excavation area. Therefore,

$$W' = \frac{(\gamma_{sat} - \gamma_w)D^2}{2} = \frac{\gamma' D^2}{2}; \quad (2)$$

$$U_s = h_{ave}\gamma_w D/2; \text{ and,} \quad (3)$$

$$FS = \gamma' D/(h_{ave}\gamma_w). \quad (4)$$

where γ_w is the unit weight of water, and γ' is the effective unit weight of soil after submerging in water.

Piping Failure Mechanism Proposed by Hsu et al.

Hsu et al. (2020) suggested that piping failure occurs locally in shear bands. When the pore spaces of brittle fracture shear bands are connected in series to form a tubular outlet pipe, the groundwater flow transitions from seepage to pipe flow. During pipe flow, groundwater carries granular soils, such as silt, sand, and gravel, upward through the tubular outlet pipe, sequentially accumulating on the excavation surface (refer to Figure 6).

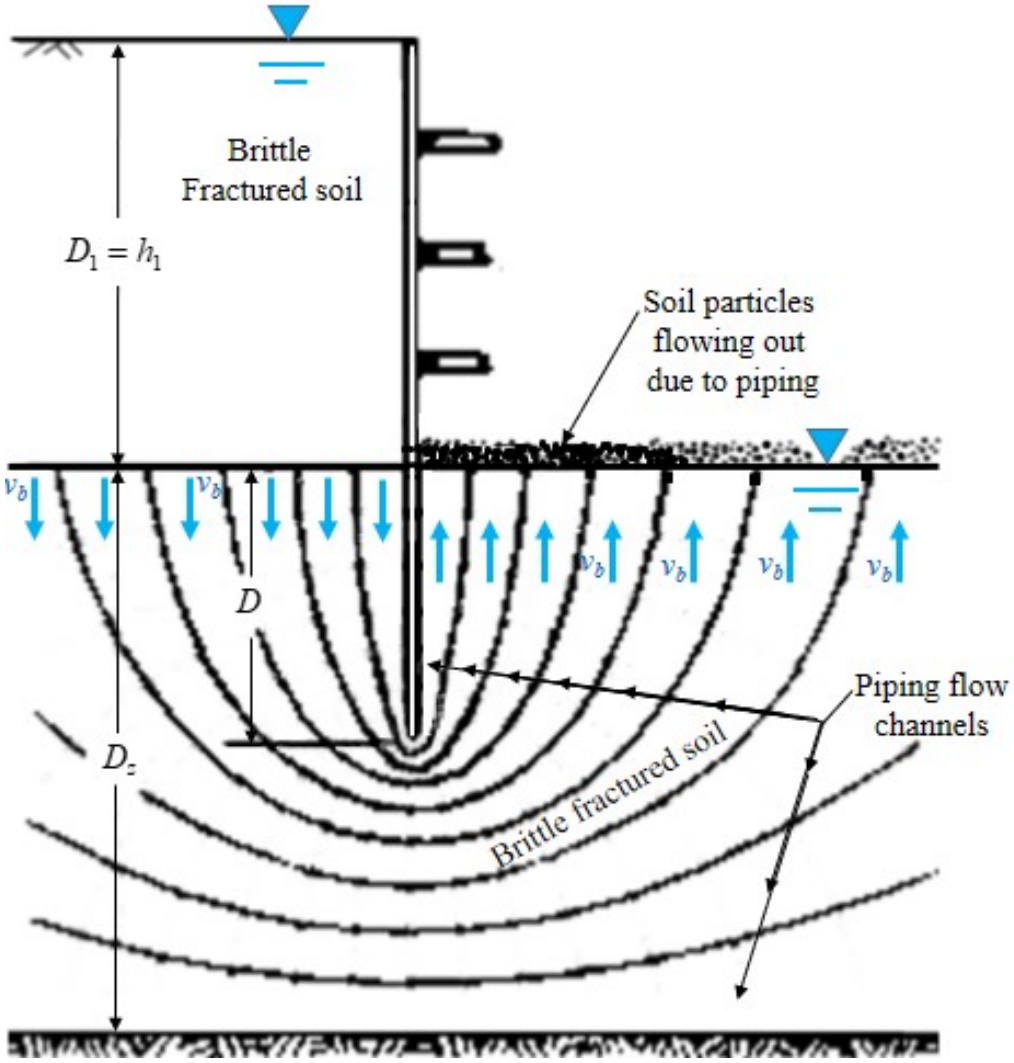

Figure 6. Piping failure of retaining wall located in shear bands under pipe flow (Hsu et al., 2020).

When pipe flow occurs in a brittle shear zone and the upward flow velocity □□ of particles within a depth D of the retaining wall below the excavation surface is greater than the critical bottom velocity □□□ required to float the soil particles, the floating soil particles will flow upward along the tubular outlet tunnel and accumulate on the excavation surface. Hsu et al. (2020) defined this phenomenon as piping.

The critical bottom velocity v_{bc} required to initiate piping failure can be

evaluated using the following formula proposed by Hsu et al. (2013):

$$v_{bc} = \sqrt{\frac{2g(G_s - 1)}{1+e}} \cdot \sqrt{D_p} \cdot \cos\beta \quad (5)$$

where g is the acceleration due to gravity, G_S denotes the specific gravity of the soils, e denotes the void ratio, D_p denotes the particle size, and β denotes the angle of inclination of the particle deposition surface.

When the size D_p of soil particles flowing sequentially in shear bands increases from 0.05 mm to 50 cm, the void ratio e of shear bands increases from 1.5 to 2.5, and when G_s is 2.65, the critical bottom velocity v_{bc} required to initiate piping failure changes depending on D_p and e, as shown in Table 1.

Table 1. Calculated critical bottom velocity for different particle sizes D_p and void ratios e (Hsu et al., 2020).

Soil classification	Particle size, D_p	Critical bottom velocity, v_{bc} (m/sec)		
		e = 1.5	e = 2.0	e = 2.5
Silt	0.05 mm	0.025	0.023	0.022
Sand	0.1 mm	0.036	0.033	0.030
Sand	0.5 mm	0.080	0.073	0.068
Sand	1 mm	0.114	0.104	0.096
Gravel	5 mm	0.254	0.232	0.215
Gravel	1 cm	0.360	0.328	0.304
Gravel	5 cm	0.805	0.734	0.680
Cobble	10 cm	1.138	1.039	0.962
Boulder	50 cm	2.544	2.322	2.150

Case Study

Problem Description

Figure 7 shows the construction site of the Jitai-Dazhi, Taipei, Taiwan, and its adjacent buildings before foundation excavation; it is clear vivid that there are two roads running in different directions and five-story buildings around the construction site.

Figure 7. Construction site and adjacent roads and buildings before foundation excavation of the Jitai-Dazhi site (Taipei, Taiwan) (Google Earth, 2023).

Figure 8 shows the collapse of the slurry wall retaining structure during the foundation excavation of the Jitai-Dazhi site. During the destruction of the slurry wall retaining structure, the slurry wall retaining structure support system was severely damaged. The building adjacent to the slurry wall retaining structure subsided notably because of lateral displacement of the foundation soil toward the excavation area, with the total subsidence amounting to approximately the height of one floor (see Figure 9).

Figure 8. Collapsed slurry wall retaining structure of the Jitai-Dazhi site during the foundation excavation.

Figure 9. Subsidence of the building adjacent to the Jitai-Dazhi site during the foundation excavation.

Figure 10 shows a cross-section of the slurry wall retaining structure used in the foundation excavation of the Jitai-Dazhi site. As illustrated in Figure 10, the foundation excavation depth D_1 is 11.95 m, and the height of the continuous retaining wall $(D_1 + D)$ is 24 m. The groundwater table behind the slurry wall retaining structure is located 4 m below the surface behind the wall (that is, h_1 = 7.95 m). The specific gravity of soil G_s is 2.65, the void ratio *e* is 1.5, the unit weight of soil after submergence in groundwater γ' is 6.47 kN/m^3, the embedded depth of the slurry wall *D* is 12.05 m, and h_{ave} is 2.98 m, as shown in Figure 5.

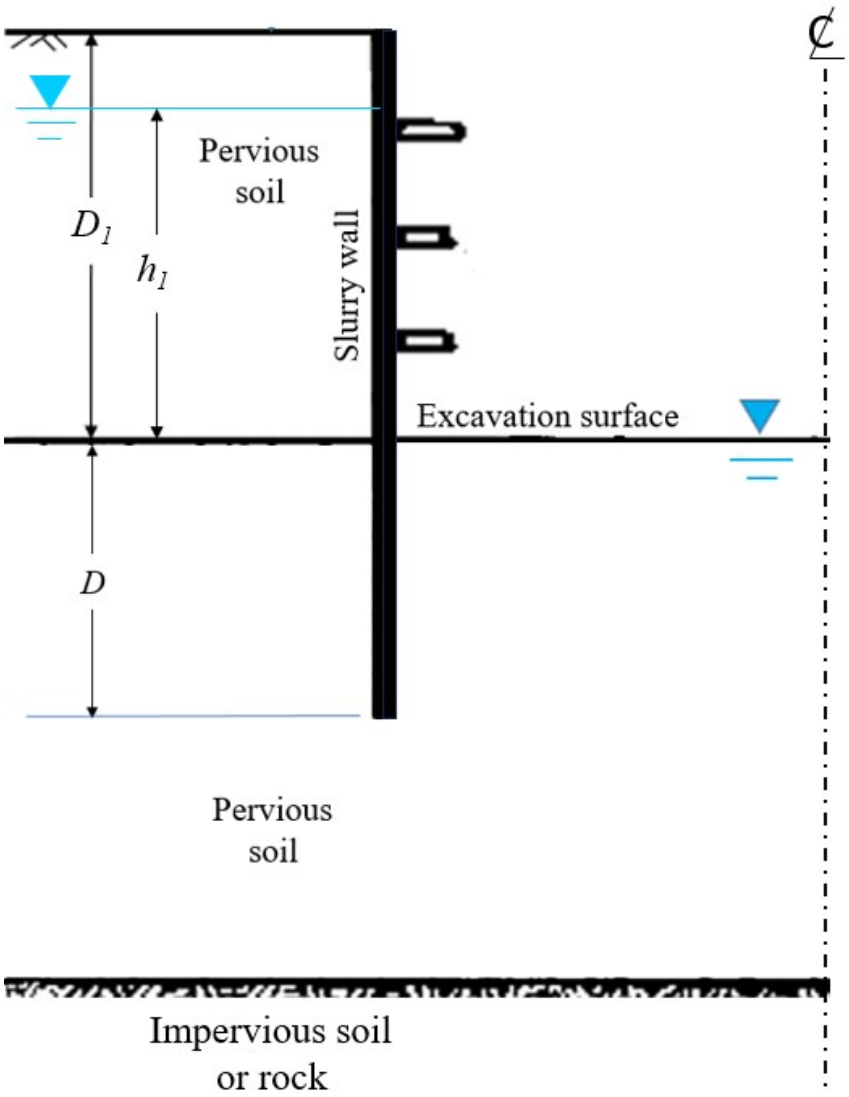

Figure 10. Sectional view of the slurry wall retaining structure used in the foundation excavation of the Jitai-Dazhi site.

Piping Failure Analyses

1) Adopting the piping failure mechanism proposed by Terzaghi

In this case study, based on the piping failure mechanism proposed by Terzaghi, the safety factor against piping can be determined as follows:

$$FS = W'/U_z = \gamma' D/(h_{ave}\gamma_w) = 2.67. \quad (6)$$

This result indicates that under the aforementioned on-site conditions, piping failure of the retaining wall will not occur during the foundation excavation for the Jitai-Dazhi site.

2) Adopting the piping failure mechanism proposed by Hsu et al.

For the construction site of the Jitai-Dazhi shown in Figure 7, the details of the slurry wall retaining structure required for foundation excavation are shown in Figure 10. Piping failure occurs under the following conditions: the groundwater table behind the slurry wall retaining structure is located 11.95 m above the excavation surface (i.e., $h_1 = 7.95$ m), the soil specific gravity G_s is 2.65, the void ratio e is 1.5, and the angle of inclination of the deposition surface of brittle-fractured soil in the shear zone β is 0°. If the pore space of shear bands is connected to form pipelines, and the efficiency coefficient E of the flow velocity of water in the tubular outlet is 1%, the calculated particle bottom velocity v_b is $E\sqrt{2gh_1} = 0.125$ m/s. Under these conditions, the bottom velocity v_b is greater than the critical bottom velocity v_{bc} for particle sizes $D_p \leq 0.1$ mm, as indicated by the data in Table 1. Therefore, granular soil, such as sand and silt, with a particle size $D_p \leq 0.1$ mm, flows upward and is deposited on the excavation surface.

When particles with sizes $D_p \leq 0.1$ mm have been discharged, the void ratio e increases from 1.5 to 2.0, and the efficiency coefficient E increases from 1% to 5%. The calculated particle bottom velocity v_b is 0.624 m/s. Under these conditions, as indicated by the data in Table 1, the bottom velocity v_b is greater than the critical bottom velocity v_{bc} for particle sizes $D_p \leq 1$ cm. Therefore, granular soil, such as sand and silt, with a particle size $D_p \leq 1$ cm, flows upward and is deposited on the excavation surface.

When particles with sizes $D_p \leq 1$ cm have been discharged, the void ratio e increases from 2.0 to 2.5, and the efficiency coefficient E increases from 5% to 10%. The calculated particle bottom velocity is 1.249 m/s. Under these conditions, as indicated by the data in Table 1, the bottom velocity v_b for a particle size $D_p \leq 10$ cm is greater than the critical bottom velocity v_{bc}. Therefore, granular soil, such as gravel, sand, and silt, with a particle size $D_p \leq 10$ cm flows upward and is deposited on the excavation surface.

Identification of Shear Bands and Shear Textures

Figure 11(a) shows an image of the area of the collapsed slurry wall retaining structure. This image, supplemented with various shear textures within the overall shear band width, facilitates the identification of key features. The collapsed area of the slurry wall retaining structure at the Dazhi-Jitai construction site reveals diverse shear textures, depicted in Figures 11(b) and 11(c), with two total shear band widths oriented along different strikes. The shear textures with distinct strikes, as illustrated in Figure 11(b), encompass principal displacement shear D with a strike of N10°W, thrust shear P with a strike of N3°E, Riedel shear R with a strike of N30°E, conjugate Riedel shear R' with a strike of N71°W, and compression texture S with a strike of N79°E. The shear textures with different trends shown in Figure 11(c) include principal displacement shear D with a strike of N72°W, thrust shear P with a strike of N46°W, Riedel shear R with a strike of N86°E, conjugate Riedel shear R' with a strike of N50°E, and compression texture S with a strike of N10°E.

(a) Before drawing the shear textures

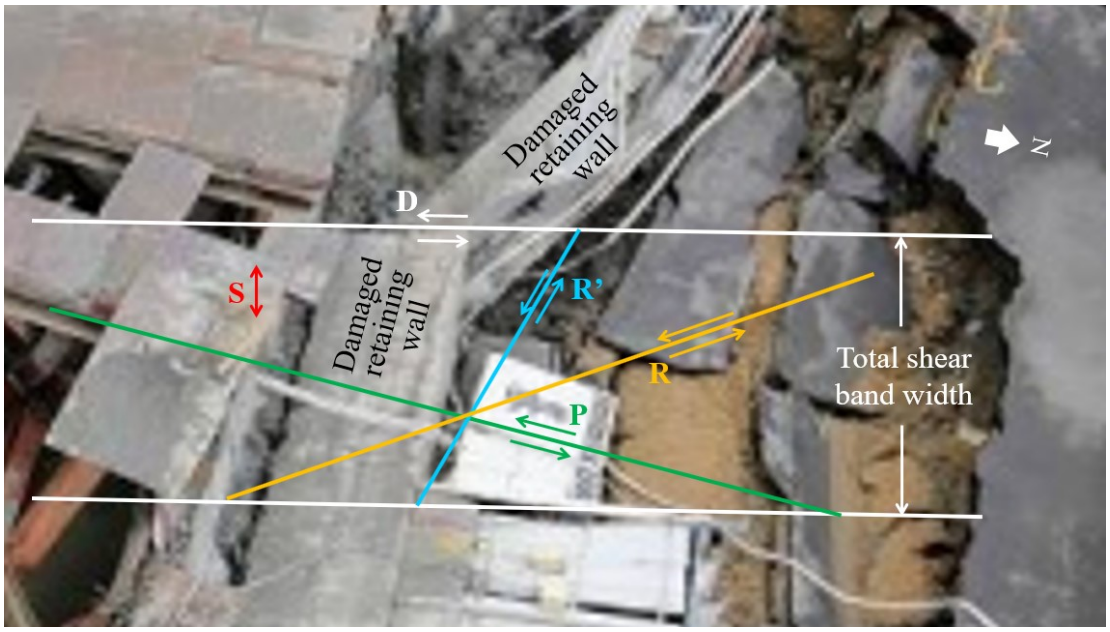

(b) After drawing the shear textures (1)

(c) After drawing the shear textures (2)

Figure 11. Identifying shear textures using an on-site image.

Comparison and Discussion

1) Figure 8 shows that during the excavation of the site of the Dazhi-Jitai, the slurry wall retaining structure collapsed severely. From Figure 8, we can see that the cause of the damage to the slurry wall retaining structure is that a large amount of soil on the back of the retaining wall was lost due to piping in shear bands, and a large piping hole appeared on the back of the slurry wall retaining structure is the topographic features of the piping failure.

2) Figure 12(a) shows that before the excavation of site of the Dazhi-Jitai, the building immediately adjacent is five-story; Figures 9 and 12(b) both show that during the excavation of the site of the Dazhi-Jitai, the adjacent building sank significantly and became a four-story building; therefore, during the excavation of the site of the Dazhi-Jitai, the adjacent buildings sank as much as one floor deep.

(a) Five stories before subsidence (Google Earth, 2023).

(b) Four stories after subsidence

Figure 12. Comparison of the number of floors before and after subsidence of the building adjacent to the Dazhi-Jitai construction site.

3) Figure 8 shows that piping failure occurred not only on the north side but also on the south side during the foundation excavation of the Jitai-Dazhi site.

4) When the slurry wall retaining structure on the north side of the Jitai-Dazhi site collapsed because of piping, a large piping hole appeared on the ground surface behind the structure due to substantial soil loss, as illustrated in Figure 8.

5) When the slurry wall retaining structure on the south side of the Jitai-Dazhi site collapsed due to piping, the building experienced substantial subsidence instead of the appearance of a large piping hole expected on the ground surface immediately behind the slurry wall retaining structure, as illustrated in Figure 12. Therefore, the formation mechanism of the large piping hole is the primary cause of the substantial subsidence of the building adjacent to the slurry wall retaining structure on the south side of the Jitai-Dazhi site.

6) For a retaining structure located in shear bands, if the backfilled soil layer continues to withstand lateral compression, the soil layer deforms locally because of strain softening when the strain penetrates the plastic range, leading to the appearance of shear bands. Soil particles in shear bands are highly oriented because of shear banding, which substantially reduces the shear resistance strength and changes steady-state, mass-conserving groundwater seepage into unsteady-state mass-non-conserving pipe flow.

7) The piping failure mechanism proposed by Terzaghi (1943) is based on groundwater seepage, which occurs comprehensively in both shear-banding and non-shear-banding areas. The piping failure mechanism proposed by Hsu et al. (2020) is based on groundwater pipe flow, and groundwater pipe flow only occurs locally in a shear banding area. Therefore, only the piping failure mechanism proposed by Hsu et al. (2020) is compatible with the local piping failure phenomenon and satisfies the requirements of hydraulic structure design.

8) For the slurry wall retaining structure at the Jitai-Dazhi site that undergoes piping failure, the safety factor against piping calculated using the formula proposed by Terzaghi (1943) is as high as 2.67. This erroneously suggests that piping failure will not occur at the site.

9) For the slurry wall retaining structure at the Jitai-Dazhi site, when the velocity v_b of groundwater flowing through soil particles in shear bands, calculated using the formula proposed by Hsu et al. (2020), is greater than the critical bottom velocity v_{bc} required to float the particles, the soil particles flow upward along the outlet pipe formed by the pore space in shear bands after being floated and are then deposited on the excavation surface. The pore

space in shear bands gradually increases after soil particles with smaller size flow out; then, soil particles with larger size also flow out, and thereafter the degree of piping failure continues to increase.

Conclusions and Suggestions

The features of the displaced landform in Taipei, Taiwan are significant. When shear bands are present at a construction site, piping failure of retaining structures occurs during foundation excavation. In this paper, the authors draw the following four conclusions by comparing the case study results of the Jitai-Dazhi excavation construction site under two different piping failure mechanisms:

1) The piping failure mechanism of retaining structures proposed by Terzaghi neglects the fact that piping failure only occurs locally in shear bands, erroneously characterizing the actual unsteady-state mass-non-conserving pipe flow required for piping failure as steady-state mass-conserving seepage.

2) Historically, technicians assessing the failure potential of retaining structures due to piping used the safety factor formula for resisting piping proposed by Terzaghi. However, the water flow conditions on which the formula was based do not satisfy the actual conditions. Therefore, the safety factor against piping obtained using the formula proposed by Terzaghi is 2.67 for the Jitai-Dazhi site. This result may lead technicians to incorrectly conclude that slurry wall retaining structure piping failure for the Jitai-Dazhi site will not occur during excavation.

3) In the piping failure mechanism proposed by Hsu et al., piping occurs when the flow velocity v_b of groundwater flowing through the bottom of particles in shear bands is greater than the critical bottom velocity v_{bc} required for floating particles. During the piping process, groundwater entrains particles of varying sizes and ejects them upward sequentially from small to large size along outlet pipes connected in series within the pore space of shear bands. Therefore, the piping failure mechanism proposed by Hsu et al. yields results consistent with the actual piping phenomenon.

4) For the foundation excavation of the Jitai-Dazhi site, when the piping failure mechanism proposed by Hsu et al. is adopted, the size of the initially ejected soil particles in shear bands is $D_p \leq 0.1$ mm, followed by particles with $D_p \leq 1$ cm, and finally particles with $D_p \leq 10$ cm. Therefore, the degree of piping failure of the slurry wall retaining structure increases with the particle size D_p of granular soils in shear bands. When slurry wall retaining structure piping failure occurs, piping holes appear on the back surface of the slurry wall retaining structure. When buildings are located behind the slurry wall retaining structure,

those located where the piping holes should appear subside significantly.

Based on these conclusions, in order to ensure that retaining walls designed by technicians remain resistant to piping failure during site excavation, the authors forward two suggestions:

1) Given that piping failure is characterized by unsteady-state mass-non-conserving pipe flow, Terzaghi's safety factor formula, based on steady-state mass-conserving seepage flow, should no longer be used in assessments.

2) The piping failure mechanism of the retaining wall proposed by Hsu et al. that satisfies practical requirements is incorporated into the retaining wall design specifications. This approach is crucial for ensuring the safety of retaining walls during foundation excavation.

References

Google Earth, Website: http://www.google.com.tw/intl/zh-TW/earth/, 2023

Hsu, Tse-Shan, Shey-En Chiu, Stephen Hsu, Cheng-Chieh Ho, "A Particle Floating Model for the Initiation of Debris Flows," *37th National Conference on Theoretical and Applied Mechanics*, 2013.

Hsu, Tse-Shan, Ming-Tuo Chen, Shey-En Chiu, "The Major Cause for the Destruction of the Gang-weigou Creek Floodway," *International Journal of Organizational Innovation,* Vol. 13, No. 2, pp. 120-143, 2020.

Terzaghi, K., Theoretical Soil Mechanics, New York, John Wiley & Sons, Inc., pp. 238-240, 1943.